Fe(II) and Co (II) Complexes of (4-(4-bromophenyl)-[2,2'-bipyridine]-6-carboxylic acid) Synthesis, Characterization and Electrochromic studies

[1]Saba*, [2]Fatima Zehra Basha, [1]Zahida Tariq Maqsood and [1]Agha Arslan Wasim
[1]Department of Chemistry, University of Karachi, Karachi, Pakistan.
[2]International Center for Chemical and Biological Sciences, University of Karachi, Karachi, Pakistan.
saba@uok.edu.pk*

Summary: In this study novel complexes of substituted bipyridine (4-(4-bromophenyl)-[2,2'-bipyridine]-6-carboxylic acid) with Fe^{+2} and Co^{+2} were synthesized and characterized by different physical, analytical and spectral techniques which includes ^{1}H-NMR, MALDI-MS, FTIR, UV-VIS Spectrophotometry, CHN analysis and conductometry. Mole ratio method revealed that both complexes satisfied ML_2 stoichiometry. Other characterization studies showed that substituted bipyridine acted as a tridentate ligand, with two pyridine N and one carboxylic O atom as binding sites per ligand molecule. The complexes were found octahedral, neutral and possessed fairly high molar absorptivities in visible region. Electrochromic studies revealed that Fe (II) complex had relatively good electrochromic properties with a reversible color change from blue to pale yellow. Co (II) complex, however, did not show significant electrochromic properties in the visible region.

Introduction

Bipyridine, a bidentate ligand, was extensively used in the development of coordination chemistry. There are different isomeric forms of bipyridine like 2,2', 3,3' 4,4'-bipyridine (symmetric) and 2,3', 2,4' 3,4'-bipyridine (asymmetric) [1]. Bipyridine has robust redox ability and it can also be easily functionalized; that is why it is studied extensively as a metal chelating agent [2]. Bipyridine is a neutral ligand and it can form charged metal complexes. The initial research on bipyridine-metal complexes was focused on the detection of metal ions in the system. It was because of the formation of highly colored complexes of metal ions with bipyridine and its derivatives [3]. However, research presently focuses on the synthesis of bipyridine derivatives possessing unique set of properties that appeal material scientists [4].

Transition metal polypyridine complexes have wide applications, ranging from biologically active materials [5-7] to photochromic and photovoltaic materials [4, 8, 9]. Transition metal complexes of bipyridine have excellent photochemical and electrochemical properties [10]. Pichos and coworkers have synthesized a series of bis-substituted bipyridines. They studied their complexes with various metal ions and reported visible electrochromism for ruthenium-bipyridine complexes [11]. Fe-bipyridine complexes showed good electrochemical properties and were used as catalyst in synthetic-organic-chemistry [12, 13]. Zhong and co-workers substituted dithienylcyclopentene on bipyridine and synthesized their iron, cobalt, and ruthenium complexes. They also studied the scope of these complexes as photo and electrochromic material to meet the demand for miniaturization of electronic components [14].

A large number of metal complexes containing substituted bipyridine ligand have been studied for their electrochromic behavior. Most of them had bipyridine as bidentate ligand. In this study, 4-(4-bromophenyl)-[2,2'-bipyridine]-6-carboxylic acid was synthesized. The synthesized ligand, anticipated as a tridentate ligand, was complexed with Fe (II) and Co (II) to study subsequent effects of polydendate ligand on their electrochromic properties. A procedure reported by Zhong [14] and Katoh [15] was modified and used to synthesize the ligand. The structure of complexes was determined using ^{1}H-NMR, MALDI-MS, FTIR, UV-VIS Spectrophotometry, CHN analysis and conductometry. Electrochemical parameters were determined using Cyclic Voltammetry and were used in spectroelectrochemical study of the complexes.

Experimental

General Experimental

The chemicals used in synthesis were reagent grade, purchased from Merck or Sigma–Aldrich and used without further purification. TLC analysis was performed using silica gel pre-coated aluminium plates (Kieselgel 60, 254, E Merck, Germany). Shimadzu 8900 IR spectrophotometer was employed to record FT-IR spectra in mid IR range,

---

400–4000 cm^{-1}, using KBr disks as sampling technique. ^{1}H-NMR were obtained using Avane Bruker 300 and 400MHz spectrometer in DMSO-d6 solvent. EI Mass spectra were obtained on JEOL MS Route 600H instrument, MALDI-MS were recorded on Bruker Daltonic – Ultra Flex III TOF/TOF, CHN (elemental) analysis was carried out on Perkin Elmer 2400 series II CHN/ S analyzer. Cyclic Voltammograms were obtained at room temperature using CH instrument 600 series. Glassy Carbon Electrode (GCE), Platinum electrode, and Ag/AgCl electrode were used as working, counter, and reference electrode, respectively. A 0.1 M solution of TetraButylAmmonium perchlorate (TBAP) in acetonitrile was used as supporting electrolyte to avoid migration current. Bulk electrolysis was performed using a custom made setup. Glassy Carbon was used as electrodes. A constant potential, measured against Ag/AgCl reference electrode, was maintained at anode using a potentiostat. Anodic and cathodic halves of electrolytic cell were physically separated using a salt bridge, saturated KNO_3 in agar gel, to avoid reduction of species oxidized at anode.

Procedure for the synthesis of 4-(4-bromophenyl)-2,2'-bipyridine-6-carboxylic acid Ligand

4-(4-bromophenyl)-2,2'-bipyridine-6-carboxylic acid was synthesized using multiple steps scheme as shown in Fig. 1 along with some modification in the synthesis procedures [14, 15].

Synthesis of 2-(bromoacetyl) pyridine **(1)**

Solution of pyridinium tribromide(39 mmol) in 150ml of glacial acetic acid was added to an ice cold solution of 2-acetyl pyridine(41 mmol) in 10.5 ml of 32%HBr solution in glacial acetic acid, and allowed to stir at 60°C for 6 hours. The reaction mixture was then cooled to room temperature. Further 300 ml of diethyl ether was added to the solution and refrigerated for 12hr at 0°C. The resulting yellow precipitates were washed using acetone and vacuum dried to obtain the product 1. Yield = 99.67%; Yellow; ^{1}H-NMR: (300MHz, CDCl$_3$): δ 8.69 (d, 1H, J = 4.2 Hz, Ar-H), 8.18 (d, 1H, J = 7.8 Hz, Ar-H), 7.89 (td, 1H, J = 7.8 Hz, J = 1.5 Hz, Ar-H), 7.54 (td, 1H, J = 4.8 Hz, J = 1.2 Hz, Ar-H), 7.61 (s, 2H, CH$_2$); EI-MS: 198.9(M^{+}), 106.0, 78.0.

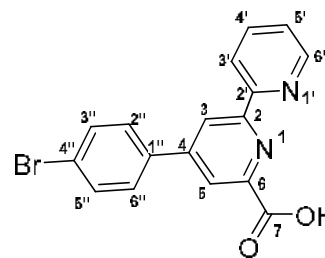*Synthessis of 2-acetyl pyridine pyridinium bromide* **(2)**

For the synthesis of 2-acetyl pyridine pyridinium bromide 50 mmol of compound 1, prepared in last step, was dispersed in THF and 5ml of pyridine was added to this solution under N$_2$

atmosphere. The mixture was stirred for 6hr at room temperature. The resulting precipitates were filtered, washed with THF, and vacuum dried to obtain product 2. Yield = 75.3%; white solid; ^{1}H-NMR (300MHz, CDCl$_3$) δ 8.99 (d, 2H, J = 5.6 Hz, Ar-H), 8.87 (d, 1H, J = 3.3 Hz, Ar-H), 8.72 (t, 1H, J = 5.7 Hz, Ar-H), 8.26 (t, 2H, J = 10.5 Hz, Ar-H), 8.15-8.06 (m, 2H, Ar-H), 7.84-7.81 (m, 1H, Ar-H), 6.49 (s, 2H, CH$_2$); EI-MS: 278.8(M^{+}), 106.0, 78.0.

Synthesis of sodium (E)-4-(4-bromophenyl)-2-oxobut-3-enoate **(3)**

A 17 ml aliquot containing 19 mmol of sodium pyruvate was added to a solution of 4-bromobenzaldehyde (17 mmol/67 ml ethanol). The suspension prepared was cooled in an ice bath, and 33ml of 10% KOH, aqueous, was added dropwise and the mixture was stirred for 2 hours. The solution became bright yellow during this stirring which was then acidified to pH 3.0 using dilute HCl. Finally, solution was filtered and the residue was washed with cold water to get product 3. Yield = 73%; Yellow solid; ^{1}H-NMR: (300 MHz, DMSO) δ 7.72 (d, 2H, J = 8.4Hz, Ar-H), 7.64 (d, 1H, J = 16.4 Hz, =CH), 7.62 (d, 2H, J = 8.4 Hz, Ar-H), 7.18 (d, 2H, J = 16.4 Hz, =CH); EI-MALDI-MS: 278.01 (M^{+}).

Synthesis of 4-(4-bromophenyl)-[2,2'-bipyridine]-6-carboxylic acid **(4)**

Stoichiometric amounts of sodium (E)-4-(4-bromophenyl)-2-oxobut-3-enoate (11.8 mmol), 2-acetyl pyridine pyridinium bromide (11.8 mmol) and ammonium acetate (94.4 mmol) were added in 83 ml water and allowed to reflux for 6 h. The precipitates formed were filtered and washed with water and acetone to get desired product 4. Yield = 39.5%; white solid; ^{1}H-NMR (300 MHz, DMSO) δ 8.70 (broad singlet, 1H, H-6'), 8.60 (s, 1H, H-3), 8.52 (d, 1H, J = 7.8 Hz, H-3'), 8.18 (s, 1H, H-5), 7.98 (t, 1H, J = 7.2 Hz, H-4'), 7.85 (d, 2H, J = 8.1 Hz, H-3'', H-5''), 7.75 (d, 2H, J = 8.1 Hz, H-2'', H-6''), 7.46 (t, 1H, J = 5.4 Hz, H-5'). MS (EI): 354.0(M^{+}), 356.9(M+2), 309 (M^{+}-COOH), 155 (bromo phenyl).
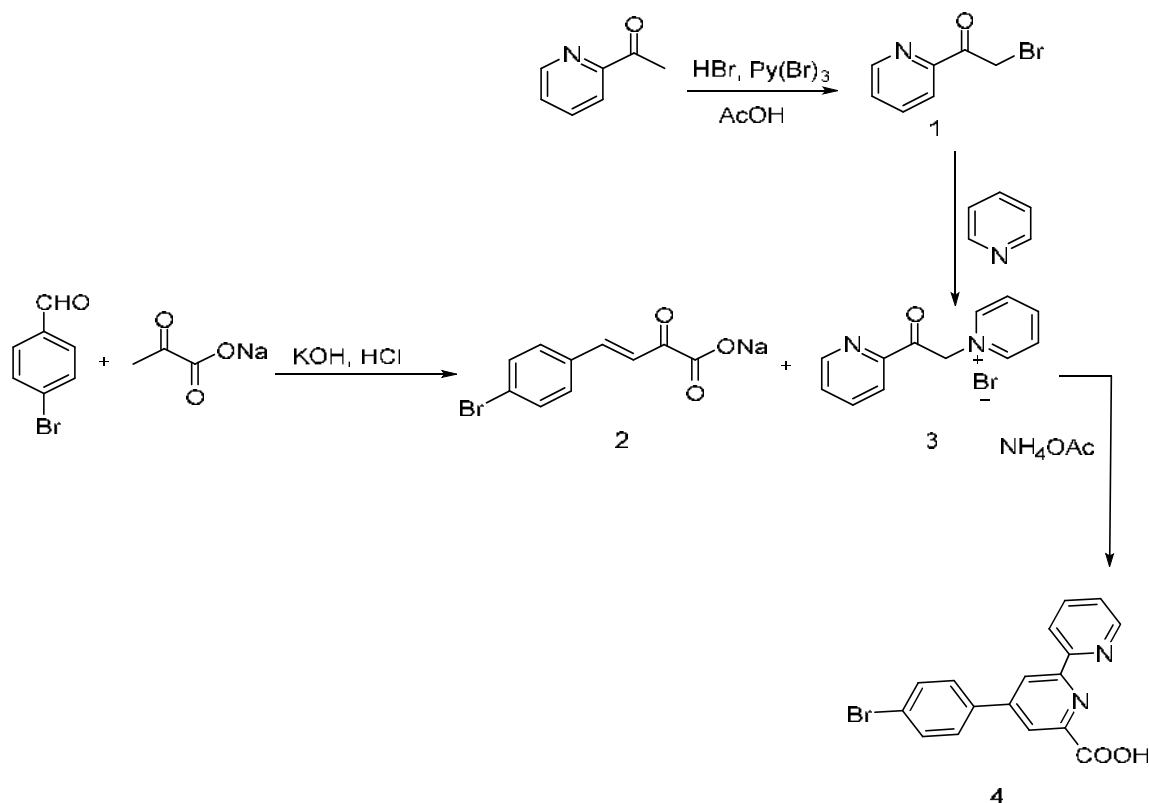
Fig. 1:   Scheme for the synthesis of 4-(4-bromophenyl)-[2,2'-bipyridine]-6-carboxylic acid.

General procedure for the synthesis of Fe and Co complex

0.1 mmol of metal chloride (FeCl₂/CoCl₂) was dissolved in 6 ml methanol. 0.2 mmol of ligand was dissolved in 4 ml methanol. The ligand solution was kept on stirring and metal solution was added gradually. The reaction mixture was stirred for further 30 min. Solid precipitates formed were filtered and washed with methanol.

Results and Discussion

Synthesis and physicochemical properties

Ligands were synthesized according to scheme shown in Fig. 1. Each product of the scheme was then characterized using spectroscopic techniques (IR, ¹H-NMR, EI-mass, MALDI). The ligand was then complexed respectively with Fe (II) and Co (II) ions and the stoichiometry of complexes was determined using mole ratio method. Both complexes satisfied ML₂ stoichiometry Fig. 2.
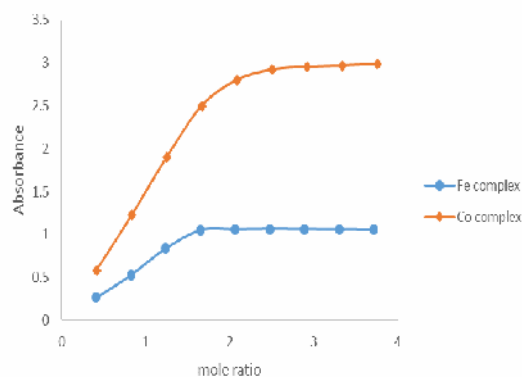

Fig. 2:   Plot of Mole ratio method for the determination of Metal-Ligand stoichiometry

The complexes were non-hygroscopic and did not show degradation at room temperature under subdued light, they were soluble in DMSO and have low solubility in DMF. Fe (II) complex was blue in color while cobalt(II) complex was yellow in color. Quick precipitation of complex was observed if complexation of metal ions and ligand was carried out using methanol as solvent. The conductivity of reaction mixture drops significantly after

complexation reaction. These observations suggest that complex is neutral/non-electrolytic in nature [16]. Presence of chloride in complex was checked by treating complex solution with AgNO$_3$. Absence of turbidity/precipitation confirmed that chloride was not present in the system. Presence of coordinated water in complex was evaluated by heating the solid complex at 110-120 °C for two hours. There was no change in the color of the complex which confirmed the absence of water in coordination sphere.

The participation of COOH group in complex formation was confirmed by a drop of pH upon stoichiometric addition of metal and ligand. The observation can be justified by the release of proton from carboxylic group of ligand after complexation; the only source of proton in the system. Further treatment of complex solution with conc. solution of strong acid resulted in disappearance of color suggesting the disintegration of complex at low pH. The complexes under study were water insoluble while they dissolved in DMSO. Water tends to dissolve compounds that have strong molecular lattice for crystal packing, like organic salts. However, such compounds have little or no solubility in DMSO. This led to interpret that the synthesized complexes either lacked strong molecular lattice or were non-ionic nature [17, 18]. Based on the above observations tentatively proposed equation for complex formation is shown in equation 1:

$$MCl_2 + 2HL \rightarrow [M(L)_2] + 2HCl \qquad (01)$$

Elemental Analysis of Complexes

The results of elemental analysis obtained using CHN analyzer are summarized in Table-1. Theoretical percentages of carbon, hydrogen and nitrogen were calculated for different metal to ligand stoichiometry values. The empirical percentages matched with the theoretical values of the proposed ML$_2$ complex stoichiometry.

Table-1: CHN - Elemental Analysis of synthesized complexes.

| Compound | %Yield | Color | Elemental Analysis | | | | | |
| | | | Observed | | | Theoretical *ML$_2$* | | |
			%C	%H	%N	%C	%H	%N
Fe Complex	83.0	Blue	53.28	2.23	7.02	53.44	2.64	7.33
Co complex	85.0	Yellow	53.50	2.48	7.15	53.22	2.63	7.30

IR Spectral Studies

IR spectral data of ligand and its complexes is reported in Table-2. IR spectrum of ligand shows an intense broad band at 3600-2000 cm^{-1}, which can

be attributed to stretching and intramolecular hydrogen bonding of carboxylic OH group. However, no broad peak was observed in IR spectra of complexes. It can be concluded with the disappearance of characteristic broad peak of carboxylic OH group that it has coordinated with the metal ion after deprotonation and was unavailable for hydrogen bonding [19, 20]. Two strong, but, merged peaks were observed in the IR spectrum of pure ligand at 1591.2 cm^{-1}. These peaks correspond to C=N and C=O stretching. The merged peaks separated into two distinct peaks after complexation [21, 22]. The shift in wavenumber for both C=O and C=N peaks also confirmed their involvement in complexation. C–N vibration frequencies also shifted towards lower wavenumbers after complexation which showed the involvement of pyridine nitrogen in complexation as well. IR studies strongly suggest that the ligand reacts with metal ions as a tridentate ligand which also favors the proposed structure for synthesized complexes.

MALDI-MS studies:

The spectral data obtained from MALDI-MS of Fe (II) and Co (II) complexes is tabulated in Table-3. Theoretical values of ion peaks were calculated using ML$_2$ stoichiometry for the two complexes. A good agreement was observed between the theoretical and empirical values which further confirmed the stoichiometry of compound.

Visible Spectral Study

Visible spectra of ligand and corresponding complexes were obtained using DMSO solvent as shown in Fig. 3. Ligand did not show absorbance in visible region but an intense peak was observed in UV region at 277.5 nm, $\varepsilon = 2.77 \times 10^4$ L mol^{-1} cm^{-1}. FeCl$_2$ spectrum was void of significant absorption peaks in the visible region. However, a weak and broad band was observed from 250 to 430nm. Fe-ligand complex exhibited charge transfer absorption band within 475-670nm, with peak at 608nm, $\varepsilon = 2900$ L mol^{-1} cm^{-1}. A strong UV absorption peak was also observed at 278 nm, $\varepsilon = 3.97 \times 10^4$ L mol^{-1} cm^{-1}.

The molar absorptivity data for ligand, metals and their complexes is tabulated in Table-4. CoCl$_2$ showed a weak absorption band in visible region within 450 – 585 nm, peak at 525 nm, $\varepsilon = 92.8$ L mol^{-1} cm^{-1}. The Co-Ligand complex exhibited charge transfer transition band within 450 – 350 nm, peak at 366.5 nm, $\varepsilon = 2238$ L mol^{-1} cm^{-1} which merged with strong UV absorption peak at 278 nm, $\varepsilon = 2.78 \times 10^4$ L mol^{-1} cm^{-1}.

Table-2: IR Spectral data of ligand and its complexes with Iron(II) and Cobalt(II).

compound	Important IR frequencies (cm⁻¹) of ligand and its complexes.					
	OH	C=O	C=N	C=C	C–N	C–O
Ligand	~3012.6 (broad band)	1591.2 (merged peak)	1591.2 (merged peak)	1425.3	1317.3	1282.6
Fe complex	~ 3415.7	1654.8/1600.8	1654.8/ 1600.8	1431.3	1303.8	1267.1
Co complex	~ 3423.4	1652.9/1602.7	1652.9/ 1602.7	1433.0	1303.8	1269.1

Table-3: MALDI-MS data of complexes.

Sample	Expected mass	Observed mass
Iron-Ligand complex	764.21 (M⁺) 676.19(M⁺- COO⁻)	764.82 (M⁺) 676.00(M⁺- COO⁻)
Cobalt-Ligand complex	767.30 (M⁺) 679.28 (M⁺- COO⁻)	767.32 (M⁺) 679.00 (M⁺- COO⁻)

Table-4: Molar absorptivities of ligand, metals and their respective complexes at $\lambda_{max.}$

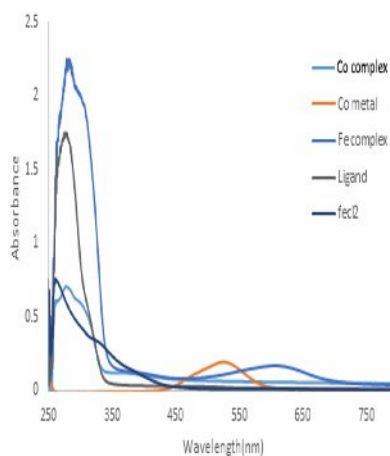| Sample	Concentration (M)	Molar absorptivities at different λ	
		Wavelength (nm)	Molar absorptivity ε (L mol⁻¹ cm⁻¹)
Ligand	6.323×10⁻⁵	277.5	27724.18
FeCl₂	3.156×10⁻³	262.2	237.96
Fe complex	5.655×10⁻⁵	278 605	39681 2900
CoCl₂	2.101×10⁻³	525	92.8
Co complex	4.333×10⁻⁵	278 366.5	27816.76 2238.39

Fig. 3: UV-Visible Spectrum of Ligand, metal, and their respective complexes.

Electrochemical studies

Cyclic voltammogram (CV) of ligand and corresponding Fe (II) and Co (II) complexes were obtained in DMSO containing 0.1M TBAP as supporting electrolyte. Only metal centered redox properties of complexes were studied because of the formation of stable redox products which showed reproducible electrochromic behavior. On the contrary, ligand centered redox products were unstable and readily revert back to their original state [23]. The pure ligand solution was found electro inactive within the selected potential window.

The cyclic voltammogram of cobalt complexes are shown in Fig. 4. The peaks observed in the voltammogram correspond to single electron transfer reaction. The peak potentials corresponds to Co(II)/Co(III) redox couple [24] which showed that redox reaction for the complex was metal centered. The value of cathodic (Epc) and anodic (Epa) peak potential, at the scan rate of 0.05 V s⁻¹, was 0.219 and 0.313V, respectively. The ideal value of ΔE for reversible single electron transfer reaction is 0.059V. However, ΔE for the reaction under study was − 0.094V which was quite far from the ideal value. This concluded that the redox reaction was not reversible. Increase in scan rate resulted in even higher ΔE separation, as shown in Table-5, which also confirmed that the complex did not show reversible redox reaction.

Table-5: Cathodic and anodic Peak potential and ΔE separation of Co complexes at different scan rate.

Sample Code	Scan rate(V/Sec)	√scan rate	Epc	Epa	Epc-Epa
Co-complex	0.05	0.2236	0.219	0.313	-0.094
	0.1	0.316	0.222	0.354	-0.132
	0.2	0.447	0.209	0.306	-0.097
	0.5	0.707	0.197	0.326	-0.129
	1	1	0.185	0.322	-0.137
	1.5	1.225	0.164	0.342	-0.178
	2.0	1.414	0.156	0.342	-0.186

Cathodic and anodic peak current of cobalt complex at 0.05 V s⁻¹ was found to be 0.8118 and − 0.5076 µA as shown in Table-6. Ipa/Ipc was 0.625 which was quite less than unity another indication that the system was not reversible. The deviation from reversibility can be attributed to the slow rate of mass and charge transfer at the electrode. The complex under study is neutral in its reduced form while upon oxidation it acquires a net positive charge. The two species can have different diffusion rates on the basis of net charge. For each voltammogram the values of Ipa was found less than Ipc suggesting slow rate of oxidation. This behavior confirms slow rate of diffusion or electron transfer for neutral complex as compared to charged oxidized complex.
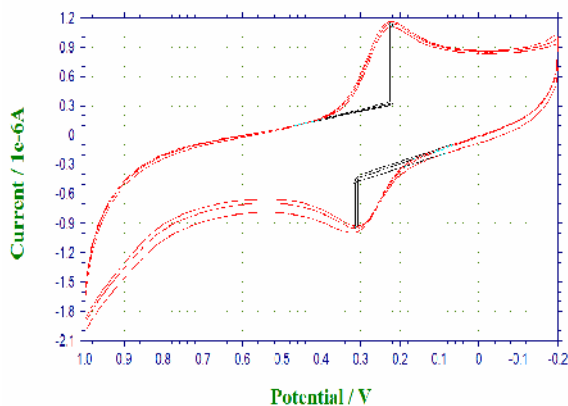
Fig. 4:   Cyclic voltammogram of Cobalt complex.

Table-6: Cathodic and anodic Peak current and their ratio for Co complexes at different scan rate.

Sample Code	Scan rate(V/Sec)	√scan rate	I_{pc} (µA)	I_{pa} (µA)	I_{pa}/I_{pc}
	0.05	0.2236	0.811	-0.507	0.625
	0.1	0.316	1.019	-0.396	0.388
	0.2	0.447	1.476	-0.949	0.643
Co complex	0.5	0.707	2.239	-1.239	0.553
	1	1	3.067	-1.364	0.445
	1.5	1.225	3.567	-1.172	0.328
	2.0	1.414	3.805	-1.097	0.288

When square root of scan rate was plotted against cathodic peak current, shown in Fig. 5, straight line was observed which indicated that redox couple was diffusion controlled.
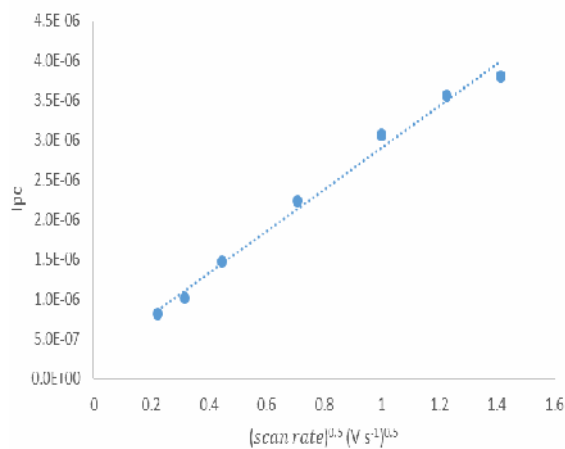

Fig. 5:   Plot of square root of scan root against cathodic peak current for cobalt complex.

It was impossible to study metal centered redox properties of Fe complex because of using DMSO as solvent. Fe complexes usually undergo redox reaction at +1.1 V [25] or higher which is outside the potential window for DMSO (-4 to +1V). A sharp increase in current was observed in CV of DMSO at potentials higher than +1V which masked the peaks of Fe complex.

Electrochromic studies

To study electrochromic behavior of the complexes, they are either oxidized or reduced and the corresponding changes in absorption spectra are studied. In this study, Chemical or electrochemical methods can be used for the oxidation or reduction of samples. In this study both chemical and electrochemical method were used. Chemical oxidation was performed by using sodium periodate solution. For electrochemical method, complexes were oxidized using bulk electrolysis at potential obtained from cyclic voltammogram for cobalt complex or literature for Iron complex [24, 25]. Cobalt complex did not show any distinct change in color upon chemical or electrochemical oxidation. Fe complex depicted significant change in UV-Vis absorption spectra upon oxidation. The color change observed was from blue (reduced) to pale yellow (oxidized) as shown in Fig. 6.
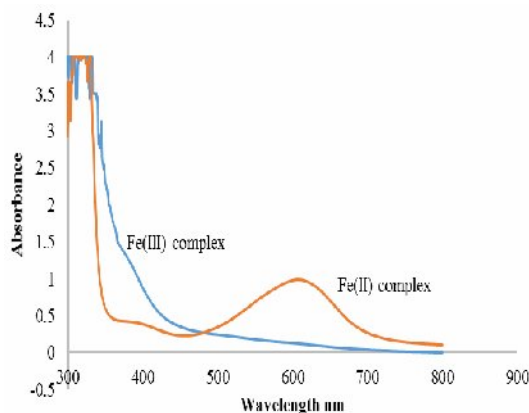

Fig. 6:   UV-Vis spectra for spectroelectrochemical study of Iron(II) complex.

Conclusion

In the present work substituted bipyridine ligand was synthesized and complexed with Fe (II) and Co (II). It was observed that the substituted bipyridine acted as a tridentate ligand. Based upon the analytical and spectral studies, the complexes had ML_2 stoichiometry. They were neutral, non-hygroscopic, and had no chloride or water molecule in the coordination sphere. The proposed structure of complexes with C_2V symmetry is shown below.
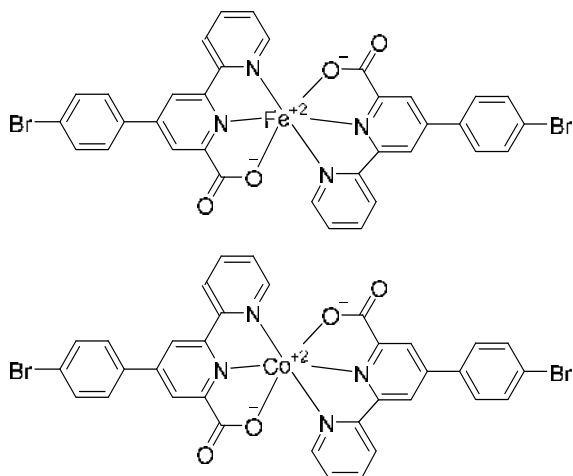
Electrochemical analysis of ligand revealed that it was electro inactive with in the applied potential window − 0.2 – 1.0V. Cobalt complex exhibit a single electron metal centered redox couple. Fe complex metal centered redox couple merged with solvent redox couple. Spectroelectrochemical studies showed that Fe complex exhibit good electrochromism with reversible color change from blue to pale yellow, while cobalt complex did not show any distinct electrochromic behavior.

Acknowledgment

References

1. C. Kaes, A. Katz and M. W. Hosseini, Bipyridine: The Most Widely Used Ligand. A Review of Molecules Comprising at Least Two 2,2'-Bipyridine Units, *Chem. Rev.*, **100**, 3553 (2000).
2. R. J. Donohoe, C. D. Tait, M. K. DeArmond and D. W. Wertz, Spectroscopic Study of the Parent and Reduction Products of Some Substituted Bipyridine Complexes of Iron(II) and Osmium(II). 2. Substitution at the 4,4'Positions, *J. Phys. Chem.*, **90**, 3927 (1986).
3. G. Maerker and F. Case, The Synthesis of Some 4,4'-Disubstituted 2,2'-Bipyridines, *J. Am. Chem. Soc.*, **80**, 2745 (1957).
4. V. Marin, E. Holder and U. S. Schubert, Polymeric Ruthenium Bipyridine Complexes: New Potential Materials for Polymer Solar Cells, *J. Polym. Sci., Part A: Polym. Chem.,* **42**, 374 (2004).
5. A. K. Gorle, A. J. Ammit, L. Wallace, F. R. Keene and J. G. Collins, Multinuclear Ruthenium (II) Complexes as Anticancer Agents, *New J. Chem.*, **38**, 4049 (2014).
6. O. M. Adelaide and O. O. James, Antimicrobial, DNA Cleavage and Antitumoral Properties of Some Transition Metal Complexes of 1, 10 – Phenanthroline and 2, 2′ – Bipyridine: A Review, *Int. J. Res. Pharm. Biomed. Sci.,* **4**, 1160 (2013).
7. T. Karabasangouda, A. V. Adhikari and G. Parameshwarappa, Synthesis of Some Biologically Active 2,4'-bipyridine-5-carbonitriles carrying the 4-hydroxyphenylthio moiety, *J. Serb. Chem. Soc.,* **74**, 733 (2009).
8. R. T. F. Jukes, B. Bozic, P. B. D. Cola and F. Hartl, Photophysical and Redox Properties of Dinuclear Ru and Os Polypyridyl Complexes with Incorporated Photostable Spiropyran Bridge, *Inorg. Chem.*, **48**, 1711 (2009).
9. R. T. Jukes, J. Kühni, N. Salluce, P. Belser, L. De Cola and F. Hartl, Photochemical, Photophysical and Redox Properties of Novel Fulgimide Derivatives with attached 2,2′-bipyridine (bpy) and [M(bpy)$_3$]$^{2+}$(M= Ru and Os) Moieties, *Dalton Trans.,* **20**, 3993 (2009).
10. R. T. F. Jukes, B. Bozic, F. E. Hartl, P. Belser and L. D. Cola, Synthesis, Photophysical, Photochemical, and Redox Properties of Nitrospiropyrans Substituted with Ru or Os Tris(bipyridine) Complexes, *Inorg. Chem.*, **45**, 8326 (2006).
11. F. Pichot, J. H. Beck and C. M. Elliott, A Series of Multicolor Electrochromic Ruthenium(II) Trisbipyridine Complexes: Synthesis and Electrochemistry, *J. Phys. Chem. A*, **103**, 6263 (1999).
12. C. Bolm, J. Legros, J. L. Paih and L. Zani, Iron-Catalyzed Reactions in Organic Synthesis, *Chem. Rev.*, **104**, 6217 (2004).
13. S. Enthaler, K. Junge and M. Beller, Sustainable Metal Catalysis with Iron: From Rust to a Rising Star?, *Angew. Chem. Int. Ed.*, **47**, 3317 (2008).
14. Y. W. Zhong, N. Vila, J. C. Henderson and H. D. Abruna, Transition-Metal Tris-Bipyridines Containing Three Dithienylcyclopentenes: Synthesis, Photochromic, and Electrochromic Properties, *Inorg. Chem.*, **48**, 7080 (2009).
15. Y. Katoh, Y. Tsujimoto, C. Yamamoto, T. Ikai, M. Kamigaito and Y. Okamoto, Chiral Recognition Ability of Cellulose Derivatives Bearing Pyridyl and Bipyridyl Residues as Chiral Stationary Phases for High-Performance Liquid Chromatography, *Polym. J.*, **43**, 84 (2011).
16. M. Teotia, D. Rastogi and W. Malik, Stereochemical Features vis-a-vis Spectral Data

on Some Nickel (II) Complexes of Amino Ligands viz. 3,3′-Diamino-4,4′-dihydroxy diphenyl sulphone and 8-amino-7-hydroxy-4-methylcoumarin, *Inorg. Chim. Acta,* **7**, 339 (1973).

17. Li Di and E. H. Kerns, In *Solvent Systems and Their Selection in Pharmaceutics and Biopharmaceutics*, Springer-Verlag, New York, p. 117 (2007).

18. A. Qurrat ul, U. Ashiq, R. A. Jamal, M. Saleem and M. Mahroof-Tahir, Alpha-Glucosidase and Carbonic Anhydrase Inhibition Studies of Pd(II)-hydrazide Complexes, *Arabian J. Chem.*, http://dx.doi.org/10.1016/j.arabjc.2015.02.024 (2015).

19. R. Mohapatra, U. Mishra, S. Mishra, A. Mahapatra and D. Dash, Synthesis and Characterization of Transition Metal Complexes with benzimidazolyl-2-hydrazones of o-anisaldehyde and furfural, *J. Korean Chem. Soc.*, **55**, 926 (2011).

20. R. Mohapatra, M. Dash, S. Patjoshia and D. Dash, Synthesis and Spectral Characterization of Transition Metal Complexes with benzothiazolyl-2-hydrazones of Salicylidene Acetone and Salicylidene Acetophenone, *Acta Chim. Pharm. Indica*., **2**, 156 (2012).

21. A. O. Adeloye, T. O. Olomola, A. I. Adebayo and P. A. Ajibade, A High Molar Extinction Coefficient Bisterpyridyl Homoleptic Ru(II) Complex with trans-2-Methyl-2-butenoic Acid Functionality: Potential Dye for Dye-Sensitized Solar Cells, *Int. J. Mol. Sci.*, **13**, 3511 (2012).

22. A. O. Adeloye and P. A. Ajibade, A High Molar Extinction Coefficient Mono-Anthracenyl Bipyridyl heteroleptic ruthenium (II) complex: Synthesis, Photophysical and Electrochemical Properties, *Molecules*, **16**, 4615 (2011).

23. B. K. Ghosh and A. Chakravorty, Electrochemical Studies of Ruthenium Componds Part 1. Ligand Oxidation Levels, *Coord. Chem. Rev.*, **95**, 239 (1989).

24. Y. W. Zhong, N. Vila, J. C. Henderson, S. Flores Torres and H. D. Abruna, Dinuclear Transition-Metal Terpyridine Complexes with a Dithienylcyclopentene Bridge Directed toward Molecular Electronic Applications, *Inorg. Chem.*, **46**, 10470 (2007).

25. Y. W. Zhong, N. Vila, J. C. Henderson and H. D. Abruna, Dithienylcyclopentenes-Containing Transition Metal Bisterpyridine Complexes Directed toward Molecular Electronic Applications, *Inorg. Chem.*, **48**, 991 (2009).